RESEARCH ARTICLE

A multielectrode array-based hypoxia model for the analysis of electrical activity in murine retinae

Claudia Ingensiep[1] | Kim Schaffrath[1] | Bernd Denecke[2†] | Peter Walter[1] | Sandra Johnen[1] iD

[1]Department of Ophthalmology, University Hospital RWTH Aachen, Aachen, Germany

[2]Genomics Facility, Interdisciplinary Center for Clinical Research (IZKF), University Hospital RWTH Aachen, Aachen, Germany

Correspondence
Sandra Johnen, Department of Ophthalmology, University Hospital RWTH Aachen, 52074 Aachen, Germany.
Email: sjohnen@ukaachen.de

Abstract

Several eye diseases, for example, retinal artery occlusion, diabetic retinopathy, and glaucoma, are associated with retinal hypoxia. The lack of oxygen in the retina, especially in retinal ganglion cells (RGCs), causes cell damage up to cell degeneration and leads to blindness. Using multielectrode array recordings, an *ex vivo* hypoxia acute model was established to analyze the electrical activity of murine wild-type retinae under hypoxic stress conditions. Hypoxia was induced by exchanging the perfusion with oxygen-saturated medium by nitrogen-saturated medium. Hypoxic periods of 0 min (control) up to 60 min were tested on the retinae of adult female C57BL/6J mice. The electrical RGC activity vanished during hypoxia, but conditionally returned after the reestablishment of conventional test conditions. With increasing duration of hypoxia, the returning RGC activity decreased. After a hypoxic period of 30 min and a subsequent recovery time of 30 min, $59.43 \pm 11.35\%$ of the initially active channels showed a restored RGC activity. The survival rate of retinal cells after hypoxic stress was analyzed by a live/dead staining assay using two-photon laser scanning microscopy. For detailed information about molecular changes caused by hypoxia, a microarray gene expression analysis was performed. Furthermore, the effect of 2-aminoethanesulfonic acid (taurine, 1 mM) on retinae under hypoxic stress was tested. Treatment with taurine resulted in an increase in the RGC response rate after hypoxia and also increased the survival rate of retinal cells under hypoxic stress, confirming its potential as promising candidate for neuroprotective therapies of eye diseases.

KEYWORDS
MEA recordings, neuroprotection, retinal ganglion cells, retinal hypoxia, taurine

1 | INTRODUCTION

Retinal hypoxia describes the lack of oxygen in the retina. It is associated with several eye diseases, for example, retinal artery occlusion, diabetic retinopathy, or glaucoma, causes damage and loss of retinal cells, and results in impairment of vision up to blindness of the patient (Osborne et al., 2004).

The retina is highly metabolically active (Winkler, 1981) and especially retinal ganglion cells (RGCs) react very sensitive to a lack of oxygen (Janaky et al., 2007; Kergoat et al., 2006), hence playing an important role in research on suitable therapies for retinal diseases associated with hypoxia. Gross et al. (1999) already showed the negative influence of short-time hypoxia on electrical RGC activity on the basis of intra- and extracellular recordings of tiger salamander RGCs.

The response of RGCs to hypoxia comprises several cellular and molecular mechanisms. Retinal hypoxia causes an increased release of vascular endothelial growth factor (VEGF) and nitric oxide synthase (NOS) (Bernaudin et al., 2002), glutamate (Kaur et al., 2006; Osborne et al., 2004), inflammatory cytokines (Arjmaa et al., 2017), and reactive oxygen species (ROS) (Block & Schwarz, 1997; Szabo et al., 1997). Under hypoxic conditions, expression of the *VEGF* gene is enhanced (Ikeda et al., 1995; Levy et al., 1995). This goes along with an increased permeability of the blood–retina barrier and leads to retinal edema (Kaur et al., 2007). Nitric oxide (NO) is also involved in vascular hyper-permeability and is increasingly synthesized due to the augmented expression of NOS (Fukumura et al., 2001). The increased release and extracellular accumulation of glutamate leads to excitotoxity, the damage and death of the affected cells by persisting overstimulation (Benveniste et al., 1984). Inflammatory cytokines are released into the damaged tissue. Chemokines recruit immune cells to the affected tissue, thus inducing an inflammatory reaction. The recruitment and subsequent infiltration of leukocytes into the inner retina leads to RGC damage (Jo et al., 2003). Furthermore, hypoxia results in a disruption of the equilibrium between pro- and antioxidants due to the accumulation of ROS. The increased production of free radicals leads to oxidative stress, which has a cytotoxic effect on the cells (Chan, 1994). Neuroprotective substances are able to prevent cellular damage caused by hypoxia. One candidate that has already been proven to possess neuroprotective next to neurotrophic and neuromodulatory effects is taurine.

Taurine (2-aminoethanesulfonic acid) is a free amino sulfonic acid. It is one of the most abundant amino acids in mammals and abounds in high concentrations in the central nervous system (Macaione et al., 1974). Taurine is involved in a multitude of physiological processes. It has a highly antioxidant effect, regulates osmotic pressure in cells, and is involved in the homeostasis of intracellular ion concentrations (El-Sherbeny et al., 2004). Regarding calcium transport, taurine plays a crucial regulatory role. At low calcium concentrations, ATP-dependent uptake of calcium ions (Ca^{2+}) is stimulated by taurine. However, taurine lowers the uptake if the

Significance

Hypoxia describes a lack of oxygen in a whole organism, an organ, or a tissue. In the eye, retinal hypoxia causes cell damage and results in vision loss. For eye diseases associated with hypoxia, analysis of the retina under hypoxic stress and establishment of therapeutic approaches to treat and prevent cell damage are of great ophthalmologic importance. Neuroprotective substances can protect cells during stress conditions and increase their survival rate. The multielectrode array-based hypoxia model established here allows for the analysis of electrical retinal ganglion cell activity before, during, and after hypoxia as well as the investigation of the effect of protective substances.

Ca^{2+} concentration is high (Pasantes-Morales & Ordonez, 1982). Ca^{2+}-dependent mitochondrial pores (mPTPs), through which apoptosis-induced factors like cytochrome c can get into the cytosol, are affected by taurine as well (Chen et al., 2009). Therefore, taurine can prevent mitochondria-mediated apoptosis. Furthermore, taurine is a neuromodulator able to prevent excitotoxicity. Because of its structural similarity to γ-aminobutyric acid (GABA), it can bind to GABA receptors and thus inhibit the excitatory effect of glutamate (Louzada et al., 2004).

Compared to *in vivo* hypoxia models, for example, laser-induced occlusion models (Martin et al., 2018; Neo et al., 2020), an *ex vivo* approach provides several advantages. Test conditions can be set more precisely and continuously monitored via sensors. The acute hypoxic effect can be directly measured, even during recovery, and the number of animals needed can be reduced due to a lower rejection rate.

The multielectrode array (MEA)-based *ex vivo* hypoxia model established here allows for the analysis of electrical RGC activity under hypoxic conditions as well as testing the effect of potentially protective substances, for example, taurine.

2 | MATERIALS AND METHODS

2.1 | Medium

Ames' medium (Sigma-Aldrich, St. Louis, Missouri) (Ames & Nesbett, 1981) was dissolved in water, then bubbled with 100% CO_2 for 30 min at room temperature (RT) and supplemented with sodium bicarbonate. It was adjusted to a pH of 7.4–7.5 and continuously bubbled with carbogen (95% O_2, 5% CO_2). For the experiments with HEPES-buffered medium, Ames' was supplemented with HEPES (Thermo Fisher Scientific, Waltham, Massachusetts) and continuously bubbled with O_2. Taurine was dissolved in Ames' medium to a final concentration of 1 mM (Chen et al., 2009; Froger et al., 2012).
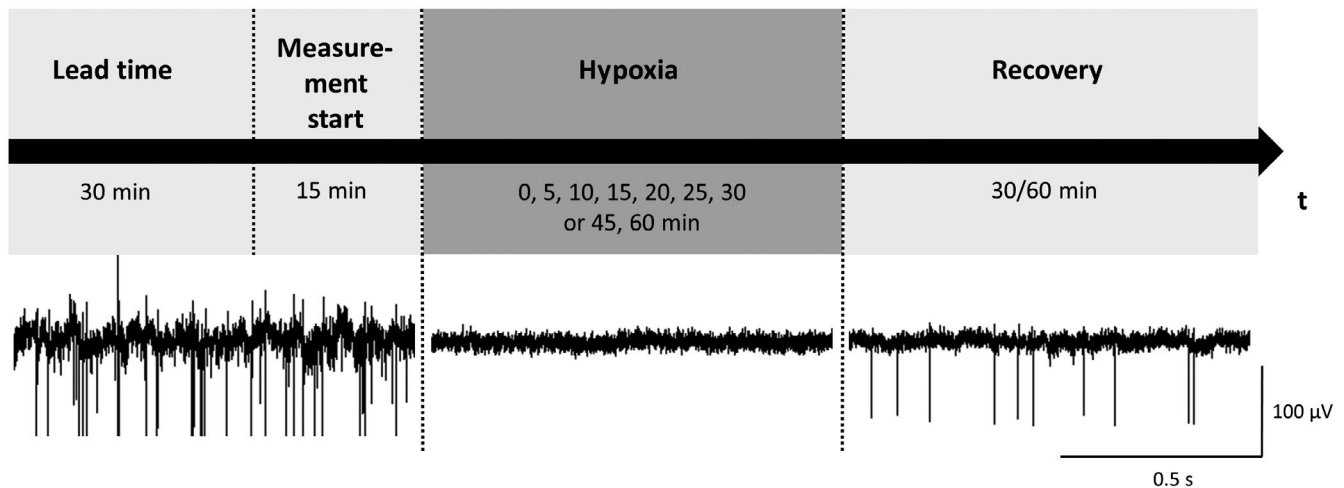
FIGURE 1 Experimental timeline for MEA recordings and depiction of characteristic RGC activity. MEA experiments started with a lead time of 30 min during which RGC activity reached a steady state. After 15 min under conventional conditions, hypoxia was induced. The hypoxic period varied from 0 min (control) to 60 min and was followed by a recovery time of 30 min (for 0- to 30-min hypoxia) or 60 min (for 45- and 60-min hypoxia). During hypoxia, the spontaneous firing of the RGCs completely vanished and conditionally returned during recovery

2.2 | Animals

Female C57BL/6J wild-type (wt) mice aged 12–20 weeks (Janvier, Le Genest-Saint-Isle, France) were kept under controlled light conditions (12:12 hr light/dark cycle), at room temperature of 21–23°C and humidity of 35%–65%, with water and food available *ad libitum* at the Institute of Laboratory Animal Science (Faculty of Medicine, RWTH Aachen University). Cages were cleaned once a week. The animals were deeply anesthetized with isoflurane (AbbVie, Wiesbaden, Germany) and killed by decapitation. All experiments were performed in accordance with the ARVO statement for the Use of Animals in Ophthalmic and Vision Research and the German Law for the Protection of Animals after approval was obtained by the regulatory authorities.

2.3 | Retina preparation

For isolation of the retinae, eyes were enucleated and directly placed into oxygen saturated Ames' medium. To guarantee sufficient oxygen supply, the tissue was transferred to fresh carbogen-bubbled medium in between different preparation steps. The left eye was pierced at the limbus with a 27 G cannula, cut radially half open, and kept in continuously carbogen-bubbled medium for later use. The right eye was opened at the limbus with an encircling cut and the anterior segment and lens were removed. The retina was carefully detached from the eye cup and separated by a cut through the optic nerve close to the optic disc. The vitreous body was carefully removed completely using forceps. The retina was cut into two halves and mounted on a nitrocellulose frame with the RGCs facing up. The frame was placed onto the electrodes of the MEA with the RGCs facing down. The second half was kept in oxygen-saturated medium

for later use. For the chip analysis and live/dead staining, both retinae were placed into a custom-designed perfusion chamber.

2.4 | MEA recording

60MEA200/30iR-Ti-pr-T type MEAs (Multi Channel Systems, Reutlingen, Germany) were hydrophilized with oxygen plasma for 2 min at 0.5 mbar in a plasma cleaner (Diener Electronic, Ebhausen, Germany). For MEA recordings, the MEA2100 system (Multi Channel Systems, Reutlingen, Germany) was used. Recording- and stimulation parameters were controlled via MC-Rack (Multi Channel Systems). To ensure the continuous perfusion with oxygen-saturated medium, a gravitation-based VC^3 perfusion system (ALA Scientific Instruments, Farmingdale, New York) was used. The inflow could be switched between four different channels. The outflow was regulated by a peristaltic pump (Gilson, Middleton, Wisconsin). The perfusion rate was set to 2.5 ml/min. To control the oxygen concentration of the medium inside the MEA ring, a fiber-optic oxygen microsensor (World Precision Instruments, Sarasota, Florida) was used. The measurement is based on the detection of oxygen concentration as a function of luminescence lifetime. One measurement per minute was taken and displayed by the OXY MICRO software (World Precision Instruments). The pH was initially monitored with indicator paper (Macherey-Nagel, Nürnbrecht, Germany) and afterward with an optic pH microsensor (World Precision Instruments). One measurement per minute was taken and displayed by the pHOptica software (World Precision Instruments).

Every experiment started with a lead time of 30 min to establish constant test conditions so that retinal firing rates reached a steady state (Figure 1). Subsequently, measurements of 70 s each were made to record the spontaneous RGC activity followed by

measurements in which the retina was electrically stimulated. Two stimulation electrodes were chosen for each experiment. The stimulation took place on one electrode at a time. A biphasic current pulse ($\pm 80\,\mu A$, 500 µs per phase, the cathodic phase preceded the anodic phase) was given every 10 s. At 45 min, hypoxia was induced. In a first model (perfusion stop model), hypoxic conditions were induced by stopping the perfusion and covering the MEA ring with parafilm. In order to define the experimental conditions more precisely, a second model (nitrogen model) was established. Here, hypoxic conditions were induced by perfusion with nitrogen saturated Ames' medium. Hypoxic periods of 0 (control), 5, 10, 15, 20, 25, 30, 45, and 60 min were tested. After hypoxia, the parafilm was removed and the perfusion restarted and nitrogen-saturated medium was exchanged by oxygen-saturated medium, respectively. In general, the hypoxic period was followed by a recovery time of 30 min. However, in experiments with 45- or 60-min hypoxia, the recovery time was extended to 60 min. If spontaneous RGC activity was detected on less than 10 of the overall 59 recording channels after 30 min lead time, no measurements were started and the retina half was rejected.

For examination of the effect of taurine, two different experimental approaches were tested. In the first approach, taurine was added at the beginning of the experiment, that is, the retina was incubated in taurine solution before hypoxia was induced (prophylactic treatment). In the second approach, taurine was added after the hypoxic period with the start of the recovery time (post-stress treatment).

In order to investigate the effect of hypoxic conditions on the excitability of RGCs in more detail, additional MEA experiments with light stimulation were performed. The animals were dark adapted for 1 hr before sacrifice. All preparation steps and MEA recordings took place in the dark under dim red light. During recording, the retina was stimulated with white light pulses (100 ms, 280 lux) every 10 s via a costume-designed LED that was connected to a stimulation panel (Roland Consult, Brandenburg an der Havel, Germany) and triggered by MC-Rack. The LED was positioned directly underneath the head stage of the MEA system, thus illuminating the retina from the RGC layer.

2.5 | Live/dead staining

In order to acquire information about the survival rate of different retinal cell types during the different test conditions, retinae were live/dead double stained and analyzed via two-photon laser scanning microscopy (TPLSM). The retinae of the *ex vivo* control, the *ex vivo* hypoxia, and the *ex vivo* hypoxia + taurine groups were treated according to the timeline of the MEA experiments in a perfusion chamber and compared to the *in vivo* status. Using the perfusion chamber instead of the MEA setup was necessary, as the retina could not be removed from the MEA electrodes without causing any damage to the tissue. In this chamber, both retinae of one animal were treated simultaneously. The tissue was placed in between two perforated plates from which it could be easily removed after the experiment.

The retinae were stained with fluorescein diacetate (FDA), staining the somata of living cells green, and with propidium iodide (PI), staining the nuclei of dead cells red. The dyes were applied for 5 min to assure that the stains penetrate the whole tissue. Subsequently, the tissue was washed three times in phosphate-buffered saline (PBS) for 5 min. To prevent bleaching, these steps were performed quickly, protected from light, and immediately before imaging.

TPLSM was carried out by a two-photon laser scanning microscope (Olympus Fluoview FV1000 MPE, Olympus Corporation, Tokyo, Japan) attached to a pulsed Ti:Sapphire laser (MaiTai DeepSee, SpectraPhysics, Santa Clara, California). A 25× NA 1.05 water dipping objective was used. For imaging the retina, a region beyond the papilla and in between the main blood vessel branches was chosen and the laser intensity was adjusted. Two stacks of subsequent images (*xy*-frames, 1,024 × 1,024 pixel) over depth (*z*, ~200 µm) with a *z*-step of 2 µm were recorded for each retina. The amount of living and dead cells in the outer nuclear layer (ONL), inner nuclear layer (INL), and ganglion cell layer (GCL) was counted using the software Imaris 9.5.0 (Bitplane, Oxford Instruments plc., Abingdon, United Kingdom), and three dimensional (3D) rendering of the image stacks was performed.

2.6 | Gene expression analysis

A transcriptome-wide gene expression analysis of retinae of four different test groups was performed by a Clariom™ D Mouse Array (Affymetrix, Santa Clara, California). Gene expression was analyzed in independent triplicate per group. Retinae were treated according to the timeline of the MEA experiments with a hypoxic period of 30 min excluding the lead time (15 min + 30-min hypoxia + 30-min recovery) without (*ex vivo* hypoxia) and with the addition of 1 mM taurine during recovery (*ex vivo* hypoxia + taurine). Control retinae were treated equally for the same time but under sufficient oxygen supply (*ex vivo* control). Additionally, freshly isolated retinae not entering an experiment were analyzed (*in vivo*) allowing for a comparison between the retinal *in vivo* and *ex vivo* status. All retinae were prepared at the same time of day in order to avoid circadian fluctuations. The experiments for the gene expression analysis were performed in a costume-designed perfusion chamber (see chapter 2.5).

Subsequently, both retinae of one animal were transferred to an Eppendorf tube forming one probe, put into liquid nitrogen and kept at −80°C until ribonucleic acid (RNA) isolation was performed using the RNeasy Mini Kit (Qiagen, Hilden, Germany) including on-column DNase digestion. Total RNA was quantified with the Nanodrop 8000 (Thermo Scientific, Waltham, Massachusetts). RNA quality was assessed using RNA 6000 Nano Assay with the 2100 Bioanalyzer (Agilent, Santa Clara, California) to ensure that the samples had a RNA integrity number (RIN) of at least 7.7. For microarray analysis, 300 ng RNA per sample was transcribed and labeled with GeneChip® WT Plus Reagent Kit according to the manufacturer's protocol (P/N 703174 Rev. 2, Affymetrix, Santa Clara, California) and hybridized to the GeneChip Clariom™ D Mouse Arrays. Hybridized

arrays were washed and stained on a Fluidics Station 450 (program: FS450 0001, Affymetrix, Santa Clara, California) and scanned on a GeneChip® Scanner 3000 7G (Affymetrix, Santa Clara, California).

2.7 | Experimental design and statistical analysis

During MEA experiments, raw data were filtered by a 200 Hz high-pass filter and a 2,000 Hz low-pass filter. The number of recording channels revealing action potentials (spikes) was counted before, during, and after hypoxia. A recording channel was classified as active if the voltage changes passed the detection threshold of −20 μV and succeeded at intervals of <5 s. These potential changes were detected in MC-Rack by the *Spike Sorter* function. The percentage of active channels after hypoxia in regard to the initial activity before hypoxia was determined. The measured activity was assigned to individual RGCs using the software Offline Sorter (Plexon, Dallas, Texas). The software sorts spikes to clusters, which correspond to individual cells, on the basis of their waveforms via principal component analysis (PCA). The data exported from Offline Sorter were processed with NeuroExplorer (Nex Technologies, Colorado Springs, Colorado), where the spontaneous firing frequency and excitability (response to a given stimulus) were analyzed. The response rate to a stimulus (at time point 0 s) was calculated by the coefficient of the pre-stimulus frequency (−3 s) and the post-stimulus frequency (500 ms). Statistical calculations and creation of the plots were performed in GraphPad Prism Version 7 (GraphPad Software Inc., San Diego, California). Significance was determined by a one-way ANOVA test with subsequent Bonferroni correction. Results are shown as mean ± standard deviation (*SD*). A *p* value ≤0.05 was considered significant. For the MEA experiments, 76 retina halves of 48 eyes (left and right) of 33 individual female mice were used. However, two mice did not enter the experiment as their retinal activity did not meet our pre-defined experimental criteria, resulting in a total animal number of 35.

Data analysis of the live/dead staining TPLSM images was performed using the Imaris 9.5.0 software. Recorded stacks were rendered in 3D and segmented into three regions of interest (ROI): ONL, INL, and GCL. Living cells (green channel) and dead cells (red channel) were automatically marked and calculated for every ROI with the *Spot* function. The number of cells/mm^2 was calculated and compared to values found in literature in order to determine the staining efficiency. Virtual sections of the image stacks in *x*, *y*, and *z* direction were made and representative examples for each group were chosen. For the live/dead staining, 16 retinae of 16 eyes (left and right) of eight individual female mice were used. However, the staining of two retinae of one mouse failed and had to be repeated, resulting in a total animal number of 9.

For the gene expression analysis, all test groups were compared to each other. Raw image data from the GeneChip® Scanner were analyzed with Affymetrix® Expression Console™ Software, and gene expression intensities were normalized and summarized with the Signal Space Transformation-Robust Multiarray Analysis

(SST-RMA) method (Irizarry et al., 2003). Statistical tests for differential expression were performed using Affymetrix® Transcriptome Analysis Console (TAC) Software, which computed and summarized a traditional unpaired one-way ANOVA for each condition group. The fold change (FC) was expressed by $\log_2$ FC in order to let reductions (negative values) and increments (positive values) center equally around 0. The gene probes were classified into significantly ($p \leq 0.05$) downregulated with FC ≤ −1.25, significantly upregulated with FC ≥ 1.25, significantly regulated with −1.25 < FC < 1.25, and not significantly regulated, and illustrated as volcano scatterplots using GraphPad Prism Version 7 (GraphPad Software Inc.). The 15 most up- and downregulated annotated genes were plotted as a heat map after hierarchical cluster analysis according to Pearson via TAC Software. In order to analyze the involved signaling pathways and functional connections of regulated genes, an enrichment analysis using the Reactome Pathway Database (Fabregat et al., 2017) was performed. For the gene expression experiments, 24 retinae of 24 eyes (left and right) of 12 individual female mice were used.

Overall, for the described experiments, a total number of 56 mice were used.

3 | RESULTS

3.1 | MEA recordings

MEA recordings of wt mouse retinae were performed before, during, and after hypoxia. To test the effect of an undersupply of oxygen on RGC activity, hypoxia was initially induced by stopping the perfusion with carbogen-saturated medium and additionally covering the MEA with parafilm (perfusion stop model). After perfusion stop, the oxygen concentration [O_2] in the medium inside the MEA continuously decreased. After 30 min, [O_2] reached a plateau at 30% of the initial [O_2]. After removing the parafilm cover and restarting the perfusion, [O_2] rapidly increased and reached the initial [O_2] in less than 10 min. Figure 2 shows a representative example of [O_2] over time during an experiment with a hypoxic period of 45 min (note that the lead time of 30 min is not included) of both hypoxia models.

Hypoxic periods of 0 min (control) up to 60 min were tested. After the perfusion was stopped, the spontaneous RGC firing decreased until it vanished completely. However, it conditionally returned during recovery time, depending on the length of the hypoxic period. The electrical RGC activity after hypoxia could differ from the initial activity before hypoxia with regard to the number of active recording channels, spike amplitude, and firing frequency. The number of recording channels on which action potentials were detected was counted before, during, and after hypoxia. One recording channel correlated with one MEA electrode. The relative number of active channels (the number of active channels after hypoxia divided by the number of active channels before hypoxia) after 30 min of recovery was analyzed (Figure 3). With increasing hypoxic period, the returning RGC activity decreased. After 30 min of hypoxia and 30 min of recovery, 52.14 ± 26.69% of the initially active channels
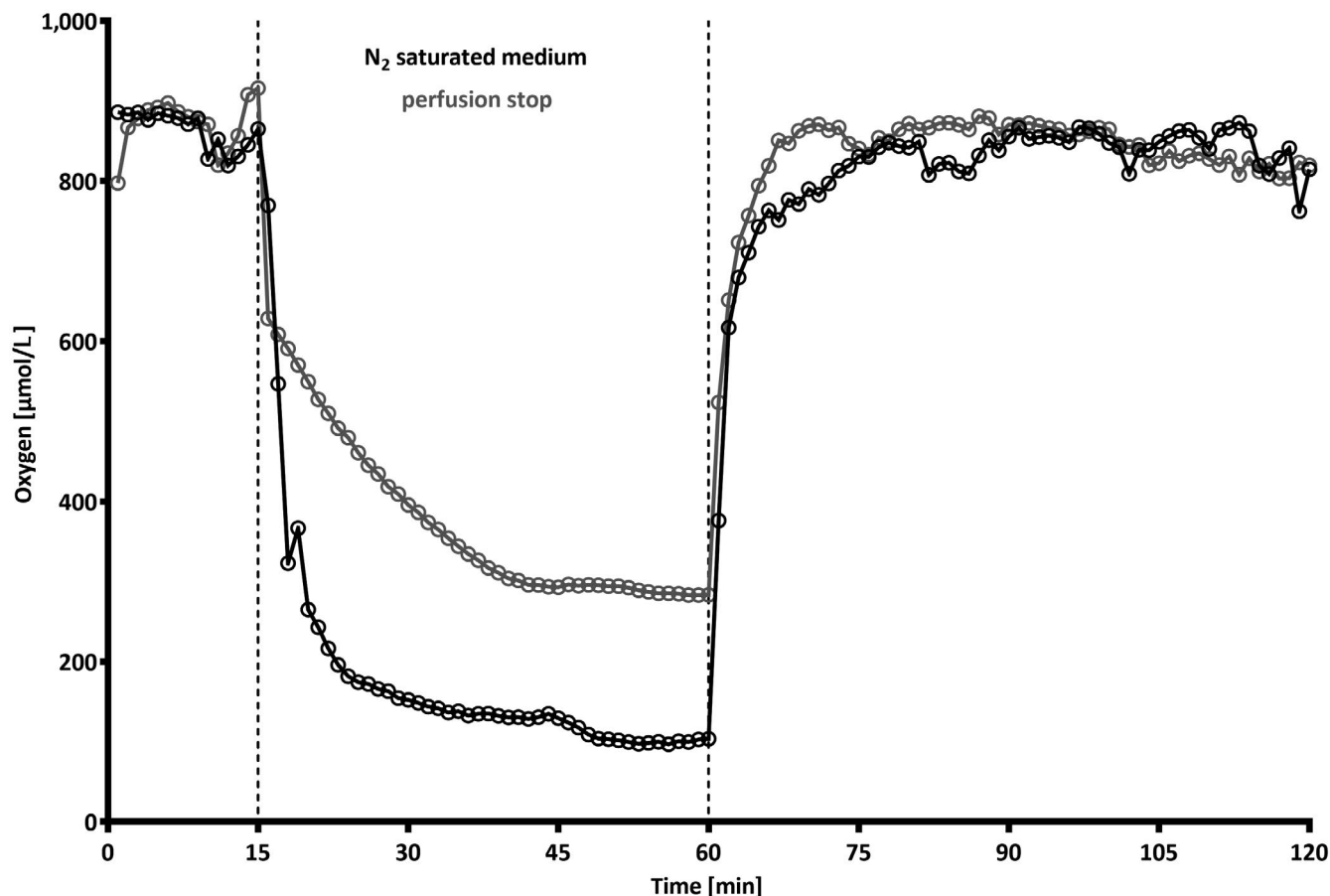
FIGURE 2 Course of O_2 concentration during a MEA experiment. Representative values of oxygen concentration in Ames' medium in the perfusion stop model (gray) and nitrogen model (black) over time (lead time is not included). Measurements were performed every minute by an optical oxygen microsensor

showed activity again. After 60 min of hypoxia, no activity returned, even after an elongated recovery time of 60 min (data not shown). A slight decrease in RGC activity over time could also be detected in the control group (96.82 ± 2.71%).

In the nitrogen model, hypoxia was induced by perfusing the retina with nitrogen-saturated medium instead of carbogen-saturated medium. During saturation with nitrogen, the carbonate buffer function was temporarily not given resulting in a slight pH increase. In order to proof that this had no effect on the experimental outcome whatsoever, additional experiments with HEPES-buffered Ames' medium and O_2 saturation were performed (data not shown). Compared to the perfusion stop model, $[O_2]$ decreased four times faster and reached a lower level (10% of the initial $[O_2]$, Figure 2). The number of active recording channels [%] after 0, 10, 20, 30, and 60 min of recovery are shown in Figure 4. As already seen in the perfusion stop model, the returning electrical RGC activity decreased with increasing hypoxic period. After 30-min hypoxia and 30-min recovery, 59.43 ± 11.35% of the active channels returned. On average, the number of active channels after 30-min recovery was 40% higher than after 10-min recovery. No activity returned after 60-min hypoxia. The returning RGC activity after short-time hypoxia was comparably high. After 10-min hypoxia, even more activity returned

compared to 5 min. However, the differences were not significant at none of the recovery points in time. The significance values for the RGC activity after 30-min recovery are shown in Table 1. For the hypoxic periods of 45 and 60 min, the recovery time was extended to 60 min, but showed no differences to 30-min recovery (data not shown).

The effect of taurine on the RGC activity under hypoxic conditions was tested using a concentration of 1 mM taurine. The optimal point in time for the addition of taurine was analyzed in two different approaches: (a) at the beginning of the experiment (prophylactic treatment) and (b) directly after the end of the hypoxic period (post-stress treatment). The second approach corresponded to the case of a possible medication with taurine after retinal damage due to hypoxia. For these experiments, a hypoxic period of 30 min was chosen due to the returning activity of about 50% in the perfusion stop model (Figure 3). Due to 26% more RGC activity after hypoxic stress without the continuous perfusion with taurine, the post-stress treatment (b) was chosen for further experiments. However, taurine showed no visible effects regarding the number of active recording channels after hypoxia, neither in the perfusion stop model nor in the nitrogen model (data not shown). Assuming that taurine may not directly affect the RGCs, but other retinal cells involved in visual
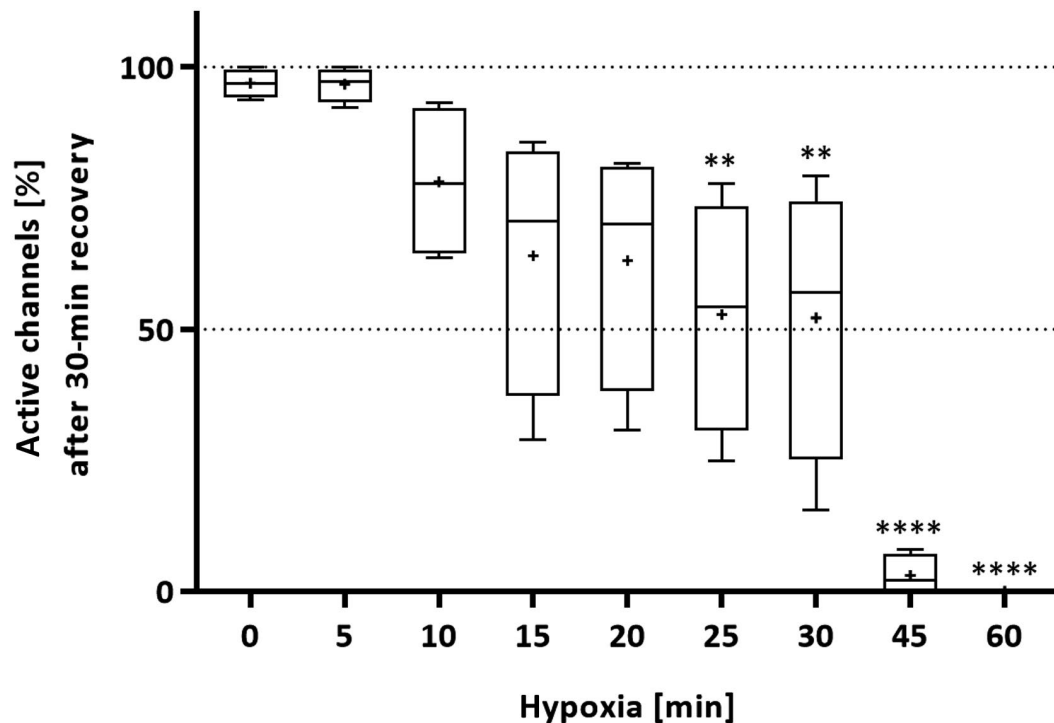
FIGURE 3 Relative RGC activity in the perfusion stop hypoxia model. Number of active MEA recording channels [%] with spontaneous RGC activity after 0- to 60-min hypoxia referring to the initial activity before hypoxia. Data are presented as box and whisker plots (whiskers: minimum to maximum, mean values indicated by +). Significant values compared to the control (0 min) are indicated by asterisks. One-way ANOVA with Bonferroni's test was performed: $F(8, 27) = 16.74$, $p < 0.0001$. Statistical analysis was performed with GraphPad Prism Software Version 7. [$n_{\text{retina halves}} = 4$/group, $n_{\text{channels}} = 11$–58/experiment, $n_{\text{recordings}} = 19$–22/experiment]

perception, experiments with light (physiological stimulus) instead of electrical stimulation were performed. The spontaneous activity and the response to light stimuli were analyzed on the following three different levels: (a) on single cell level after spike sorting, (b) on recording channel level comprising all active channels, and (c) on recording channel level comprising only those channels that showed activity after hypoxia, too (Figure 5). On all analysis levels, the spontaneous RGC activity was always lower after hypoxia than before, regardless if under Ames' medium or under the addition of taurine. Additionally, there was no significant difference between Ames' and taurine before or after hypoxia, respectively. The spontaneous firing frequency on cell level decreased by 53% from 12.07 ± 13.68 Hz before hypoxia to 5.73 ± 6.12 Hz after 30-min hypoxia and 30-min recovery under Ames' and by 54% from 13.70 ± 14.71 to 6.24 ± 8.24 Hz under taurine (Figure 5a). On channel level, the firing frequency dropped by 78% from 27.13 ± 28.02 to 5.93 ± 6.83 Hz under Ames' and by 84% from 38.84 ± 40.46 to 6.1 ± 11.92 Hz under taurine (Figure 5b). On channel level (direct comparison), the firing frequency declined by 88% from 48.07 ± 30.37 to 5.93 ± 6.83 Hz under Ames' and by 90% from 58.75 ± 42.57 to 6.1 ± 11.92 Hz under taurine (Figure 5c). Analyzing the response rate, the effect of taurine became more distinct with every analysis level (Figure 5d–f). The RGC response rate was increased under taurine after hypoxia on both cell level (Figure 5d) and recording channel level (Figure 5e,f). On channel level (direct comparison, Figure 5f), the response rate

under Ames' after hypoxia was significantly increased as well (factor 1.7), although significantly lower than under taurine (factor 3.8).

3.2 | Live/dead staining

In order to differentiate whether inactive RGCs after hypoxia did not fire because they were alive but still in a silent stress mode or whether they were already dead, live/dead stainings were performed. The retinae of different culture conditions (*in vivo*, *ex vivo* control, *ex vivo* hypoxia, *ex vivo* hypoxia + taurine) were stained with FDA and PI. The stacks of TPLSM images were analyzed both qualitatively and quantitatively (Figure 6). The scanning throughout the whole retina enabled the differentiation between the different retinal layers and allowed for counting the amount of dead cells in the ONL, INL, and GCL. In the *in vivo* group, only single dead cells could be detected. The amount of dead cells in retinae which underwent 30-min hypoxia was significantly increased compared to the control groups (6.4-fold compared to the *in vivo* group and 3.4-fold compared to the *ex vivo* control group, Figure 6c). The number of dead cells after hypoxia was lower in the presence of taurine (47% lower for ONL, 37% for INL, and 25% for GCL), even though not significantly. The photoreceptors forming the ONL were the least hypoxia-affected retinal cells. In all test groups, the majority of dead cells was located in the GCL. Since the staining did not always penetrate ONL
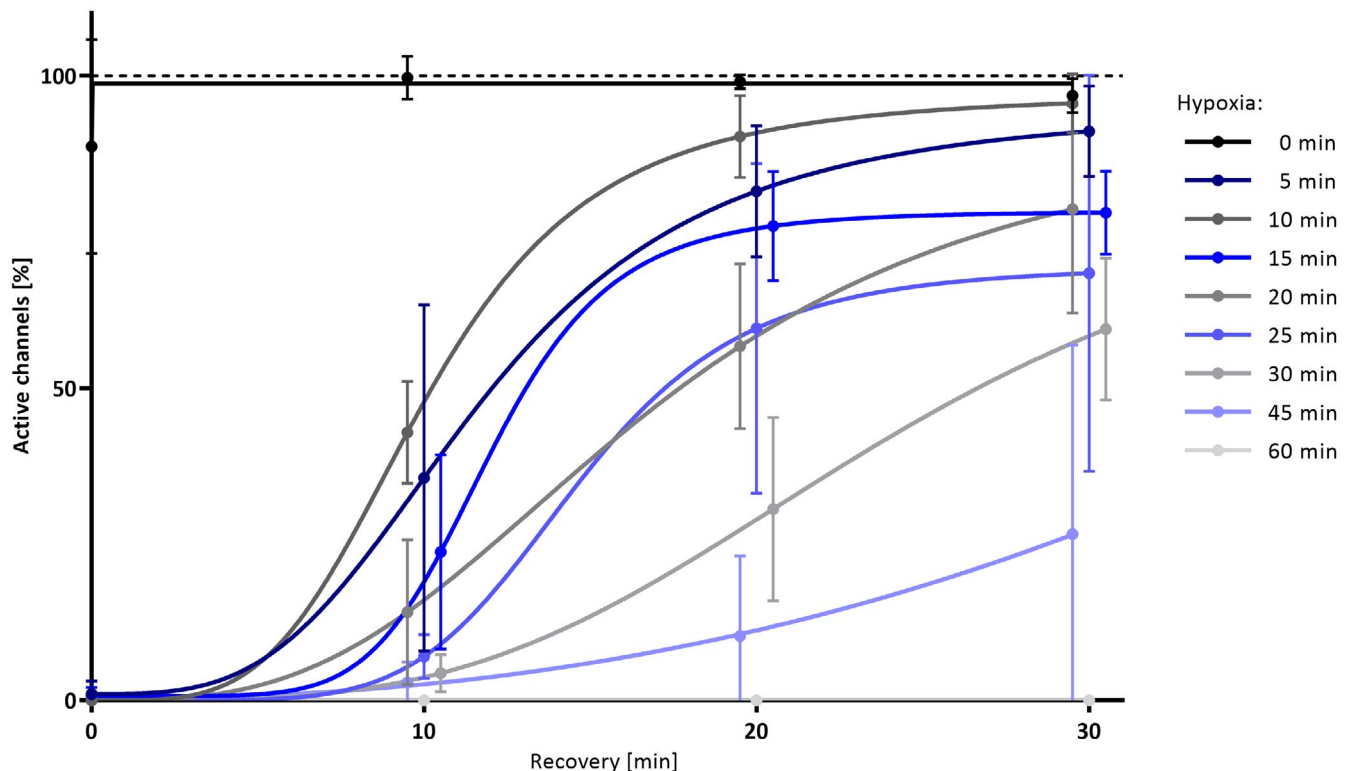
FIGURE 4 Relative RGC activity in the nitrogen hypoxia model. Number of active MEA recording channels [%] with spontaneous RGC activity after hypoxia referring to the initial activity before hypoxia. The returning RGC activity after 0- to 60-min hypoxia is shown after 0, 10, 20, and 30 min of recovery. For better graphical clarity, the data points and error bars are slightly shifted to the left and to the right. Data are presented as mean $\pm$ SD. One-way ANOVA with Bonferroni's test was performed: $F(8, 27) = 15.98$, $p < 0.0001$. Statistical analysis was performed with GraphPad Prism Software Version 7. [$n_{\text{retina halves}}$ = 4/group, n_{channels} = 15–52/experiment, $n_{\text{recordings}}$ = 16–23/experiment] [Color figure can be viewed at wileyonlinelibrary.com]

and INL equally well, relative cell numbers were only calculated for the properly stained GCL (Figure 6d). According to literature values (Jeon et al., 1998), about 70% of the cells in the GCL were stained. The relative number of dead cells in the *ex vivo* groups was significantly higher compared to the *in vivo* retinae. The highest amount of dead cells was found in the *ex vivo* hypoxia group (84.72% $\pm$ 12.63%). The addition of taurine had a positive, though not significant, effect on the survival rate of the cells in the GCL (73.13% $\pm$ 11.91%).

3.3 | Gene expression analysis

The retinal transcriptome was analyzed by microarrays. In order to get a more detailed insight into the molecular changes and the effects taurine has on the retina under hypoxic conditions, four different test groups were analyzed—*in vivo*, *ex vivo* control, *ex vivo* hypoxia, and *ex vivo* hypoxia + taurine. The results of the gene expression analysis of the different test groups were compared among each other, and up- and downregulated genes were identified (Figure 7). The negative $\log_{10}$ of the p value was plotted against the $\log_2$ of the FC to visualize how many genes as well as how significantly the genes were up- or downregulated. The retinal gene expression profile revealed much bigger differences between the *in vivo* group and the three *ex vivo* groups than among the *ex vivo* groups themselves.

Compared to the *in vivo* status, 4.24% of the genes were significantly upregulated and 2.28% significantly downregulated in the *ex vivo* control group (Figure 7a), 2.17% were significantly upregulated and 1.65% downregulated in the *ex vivo* hypoxia group (Figure 7b), and 2.76% were significantly upregulated and 2.12% downregulated in the *ex vivo* hypoxia + taurine group (Figure 7c). Compared to the *ex vivo* control, 1.75% of the genes were significantly upregulated and 0.98% downregulated in the *ex vivo* hypoxia group (Figure 7d), and 2.64% were significantly upregulated and 1.21% downregulated in the *ex vivo* hypoxia + taurine group (Figure 7e). The comparison of both hypoxia groups revealed that 0.97% of the genes were significantly upregulated and 0.63% were downregulated in the *ex vivo* hypoxia + taurine group (Figure 7f).

The most regulated coding genes are shown in Figure 8a. Comparing the gene expression profile of the *ex vivo* retinae with the *in vivo* status, several immediate early genes (IEGs) were identified, representing the first response to a stimulus before new protein synthesis takes place. The genes *Cyr61*, *Fosb* (Figure 8b), and *Fos* represented the top regulated IEGs. However, the differences in between the *ex vivo* groups were very small. Taurine had an effect on the expression of several genes. For example, the gene *Knip3*, coding for the potassium voltage-gated channel interacting protein 3, was significantly downregulated in the *ex vivo* hypoxia + taurine group compared to the *ex vivo* hypoxia group. Furthermore, the expression

TABLE 1 Significance values of the relative RGC activity in the nitrogen hypoxia model after 30-min recovery

Hypoxia [min]	0	5	10	15	20	25	30	45	60
0		ns $p > 0.9999$	ns $p > 0.9999$	ns $p > 0.9999$	ns $p > 0.9999$	ns $p = 0.7854$	ns $p = 0.1257$	**** $p < 0.0001$	**** $p < 0.0001$
5			ns $p > 0.9999$	ns $p > 0.9999$	ns $p = 0.9999$	ns $p = 0.9999$	ns $p < 0.4135$	*** $p = 0.0003$	**** $p < 0.0001$
10				ns $p > 0.9999$	ns $p > 0.9999$	ns $p > 0.9939$	ns $p = 0.1635$	**** $p < 0.0001$	**** $p < 0.0001$
15					ns $p > 0.9999$	ns $p > 0.9999$	ns $p > 0.9999$	** $p = 0.0054$	**** $p < 0.0001$
20						ns $p > 0.9999$	ns $p > 0.9999$	** $p = 0.0047$	**** $p < 0.0001$
25							ns $p > 0.9999$	* $p = 0.0483$	*** $p = 0.0001$
30								ns $p = 0.3282$	*** $p = 0.0009$
45									ns $p > 0.9999$
60									

Note: Statistical analysis was performed with GraphPad Prism Software Version 7.

profile of the gene *Ptgds*, coding for glutathione-independent prostaglandin D synthase, in the taurine group resembles more the *ex vivo* control than the *ex vivo* hypoxia group. However, genes that are generally known to be regulated during hypoxic conditions, for example, *Hif1a* (Figure 8b) and *VEGFA*, were not significantly regulated under the selected experimental conditions.

Comparing the *ex vivo* retinae to the *in vivo* status, the enrichment analysis, showing regulated pathways, revealed cellular responses to external stimuli (ID: R-MMU-8953897, Reactome 2019) and stress (ID: R-MMU-2262752, Reactome 2019) as well as oxidative stress-induced senescence (ID: R-MMU-2559580, Reactome 2019) (data not shown).

4 | DISCUSSION

Hypoxia is a serious complication resulting in cell damage up to cell death. Here, we have shown that it had an immense effect on the electrical firing behavior of RGCs and their survival rate. The spontaneous RGC activity vanished during O_2 undersupply, but conditionally returned after the reestablishment of conventional conditions. The amount of returning activity depended on the hypoxic period length. With increasing hypoxic period, the returning RGC activity decreased. Whereas the RGC activity changed only marginally after 5 and 10 min of hypoxia, the effects of O_2 suppression became more clearly after elongated hypoxic periods. The returning RGC activity changed in the number of firing cells, the firing rate, spike amplitude, and the response rate to given stimuli. Every MEA electrode can measure the activity of not only one, but several cells. Therefore, spike sorting was mandatory in order to analyze the firing behavior on single cell level. Recorded spikes were clustered and assigned to single cells by means of their waveform. For activity clusters could not always be distinguished unmistakably, some spikes remained unsorted, so that information got lost during this process. Therefore, RGC activity was not only analyzed on single cell, but also on recording channel level. All these data combined provided a more comprehensive view on the RGC activity.

However, the results presented here were obtained from female mice only, thus a gender-specific effect cannot be excluded.

Regarding previous research on the electrical activity of RGCs under hypoxic stress, intra- and extracellular recordings were performed. Gross et al. (1999) analyzed RGC activity under hypoxic conditions in single-unit extracellular and whole-cell voltage clamp experiments. After light stimulation, their results showed an OFF response suppression in the tested ON-OFF RGCs under hypoxia. The ON responses, however, were only slightly affected. They also showed that short-time hypoxia (15 min), which had a negative effect on the RGC firing behavior, was reversible. In contrast, long-term hypoxia and the concomitant increase in the glutamate level caused irreversible cell damages (Dreyer et al., 1996).

The decline in RGC activity showed the cells' transition into stress mode. RGCs react highly sensitive to hypoxic conditions, which is due to their high metabolic activity. In order to save energy, the spontaneous firing as well as the response to stimuli is closed down. This effect is conditionally reversible. The RGCs could recover from short-time hypoxia after reestablishing the conventional test conditions with sufficient O_2 supply. RGCs that remained inactive during recovery time could either still be

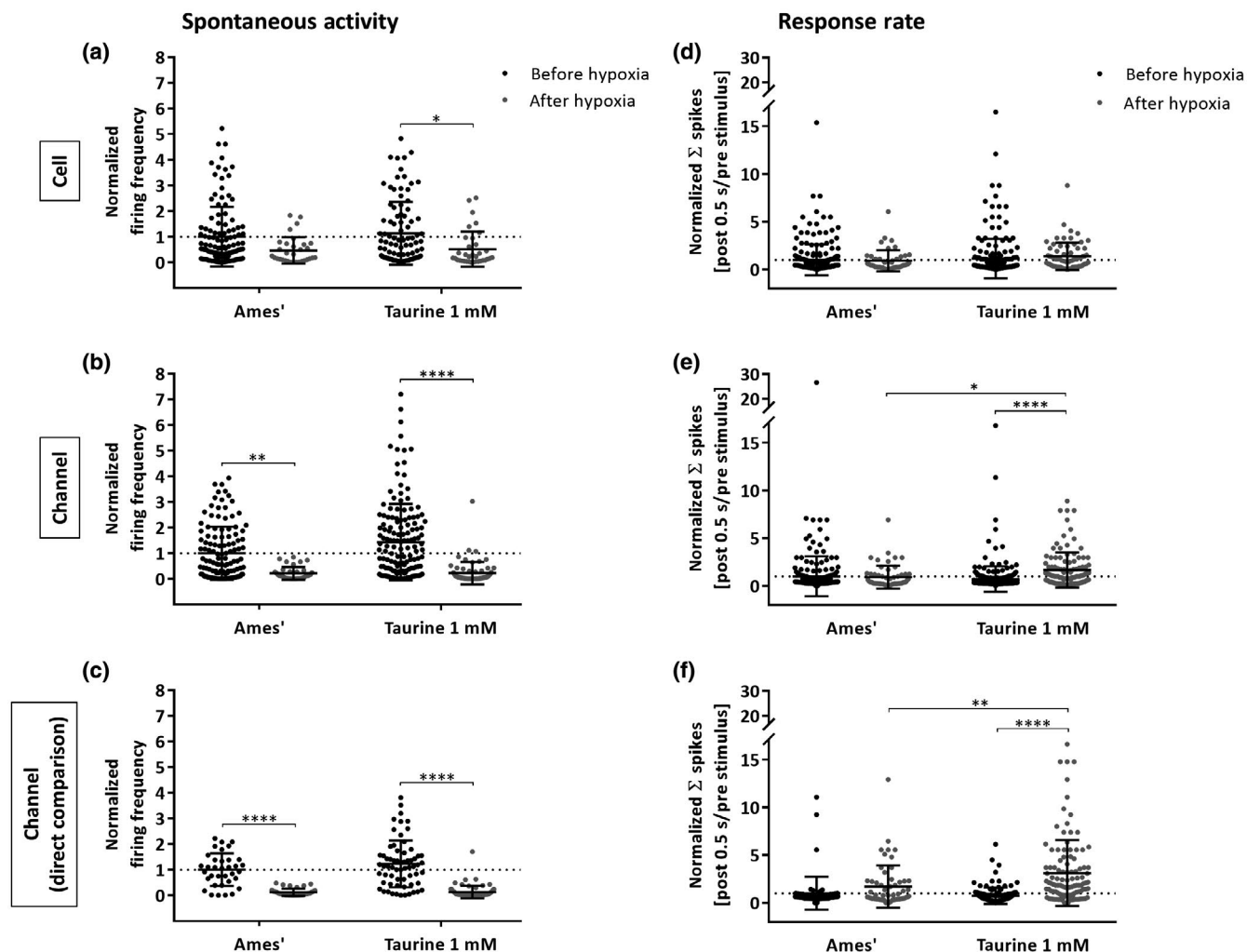## Spontaneous activity

Response rate

FIGURE 5 Spontaneous activity and response rate to light stimulation of RGCs in the nitrogen hypoxia model. (a–c) The spontaneous firing frequency [Hz] and (d–f) response rate to light stimulation of RGCs during MEA experiments before and after 30-min hypoxia under Ames' medium and after addition of taurine (1 mM). (a) Normalized spontaneous activity after spike sorting on single cell level, (b) on recording channel level, and (c) on recording channel level considering only channels with RGC activity before and after hypoxia. The firing frequency under Ames' medium before hypoxia was set to 1. (d) Normalized response rate after spike sorting on single cell level, (e) on recording channel level, and (f) on recording channel level considering only channels with RGC activity before and after hypoxia. The response rate was defined by the coefficient of the number of spikes 500 ms after stimulus and 3 s before stimulus. The response rate under Ames' medium before hypoxia was set to 1. Data are presented as scatterplots with mean $\pm$ SD. Significant values are indicated by asterisks. One-way ANOVA with Tukey's test was performed: a: $F_{(3, 279)} = 5.04$, $p = 0.0020$; b: $F_{(3, 376)} = 22.98$, $p < 0.0001$; c: $F_{(3, 196)} = 51.09$, $p < 0.0001$; d: $F_{(3, 545)} = 1.04$, $p = 0.3763$; e: $F_{(3, 700)} = 8.478$, $p < 0.0001$; f: $F_{(3, 361)} = 23.21$, $p < 0.0001$. Statistical analysis was performed with GraphPad Prism Software Version 7. [$n_{retina\ halves}$ = 4/group, $n_{channels}$ = 23–50/experiment, n_{cells} = 6–61/experiment, $n_{recordings}$ = 20/experiment]

in stress mode or irreversibly damaged and apoptotic. In order to differentiate between these two phases and define the number of cells that were already dead, live/dead staining and TPLSM were performed. In all groups, most of the dead cells were located in the GCL, followed by the INL, whereas in the ONL only single dead cells were found. In all layers, the highest number of dead cells was found in the *ex vivo* hypoxia group. The amount of dead cells in the GCL of the *ex vivo* hypoxia retinae was significantly increased compared to the *in vivo* retinae. The *ex vivo* control and the *ex vivo* hypoxia + taurine retinae revealed, though to a lower significance level, a straining effect of the artificial conditions themselves and

a slight neuroprotective effect of taurine on the cells' survival rate, respectively.

Analyzing the survival of RGCs under hypoxic conditions, several studies worked with cell cultures in the so-called hypoxia chambers (Hong et al., 2007). These chambers allowed for a precise composition of O_2, CO_2, and N_2. Chen et al. (2009) worked with the RGC-5 cell line and exposed the cells to hypoxia in a culture chamber with 5% O_2, 5% CO_2, and 90% N_2 at 37°C testing the effect of taurine (0.01, 0.1, and 1 mM) on the apoptotic rate. After pretreating the cells with taurine (1 mM) and 48 hr of hypoxic conditions, the survival rate increased from 49% (untreated) to 63%. A comparison of
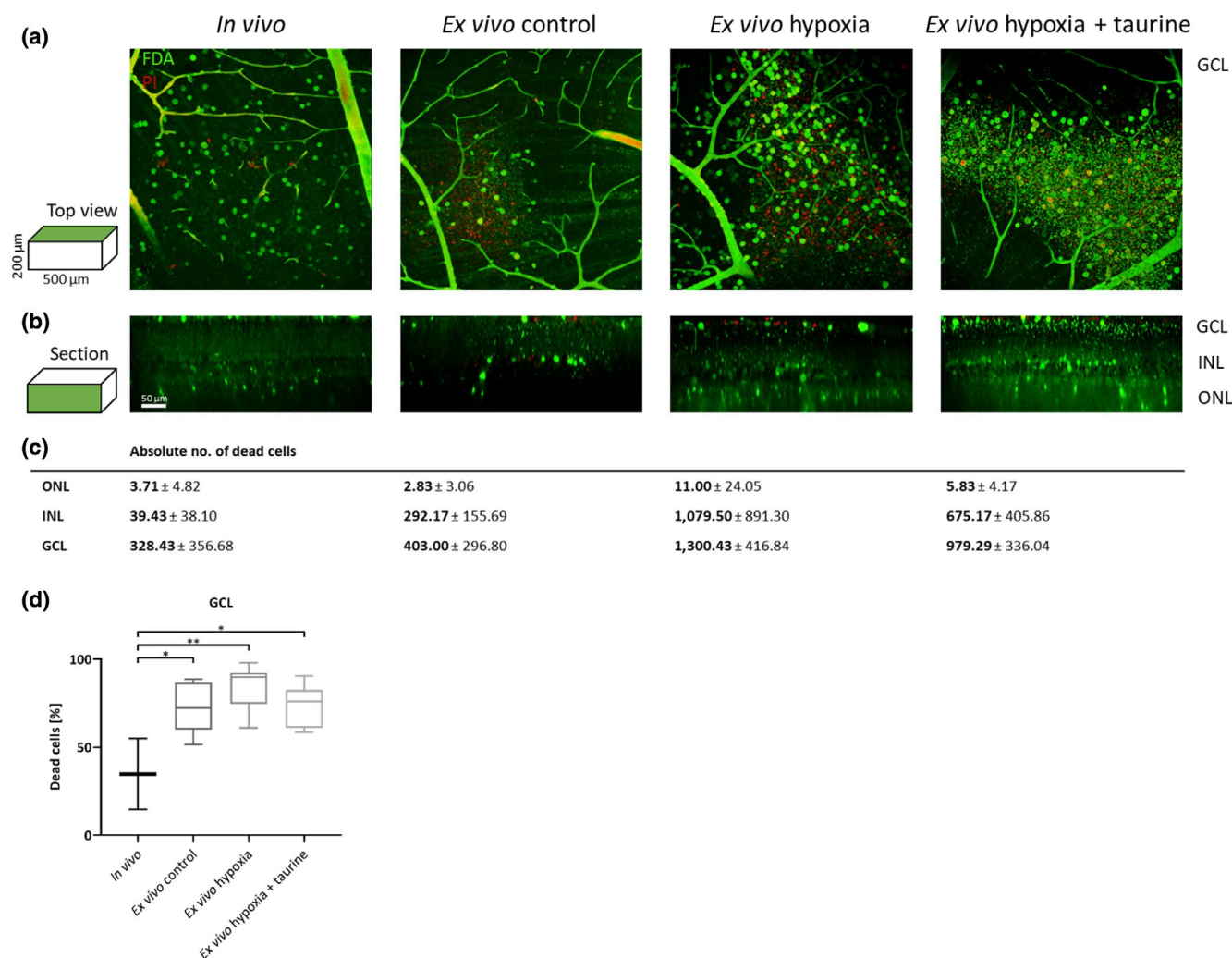
FIGURE 6 TPLSM-based analysis and quantification of live/dead stained retinae. Retinae at different culture conditions (*in vivo*, *ex vivo* control, *ex vivo* hypoxia, and *ex vivo* hypoxia + taurine) were stained with fluorescein diacetate (FDA) and propidium iodide (PI). FDA stains the somata of living cells green, PI stains the nuclei of dead cells red. Images were taken by a two-photon microscope (Olympus Fluoview FV1000 MPE). (a) Top view onto ganglion cell layer (GCL). (b) Section through the retina. (c) Absolute number of dead cells in the outer nuclear layer (ONL), inner nuclear layer (INL), and ganglion cell layer (GCL). (d) Relative number of dead cells in the GCL. Cell quantification was performed using Imaris Software. Data are presented as box and whisker plots (whiskers: minimum to maximum). Significant values are indicated by asterisks. One-way ANOVA with Tukey's test was performed: $F(3, 17) = 6.32$, $p = 0.0045$. Statistical analysis was performed with GraphPad Prism Software Version 7 [$n_{\text{retinae}} = 4$/group] [Color figure can be viewed at wileyonlinelibrary.com]

our results to primary RGCs and retina explants is more appropriate. Furthermore, van Bergen et al. (2009) stated that cells designated as RGC-5 should be first analyzed by confirming the species to be of rat origin and retinal-specific marker expression. Tan et al. (2011) isolated RGCs from Sprague-Dawley rats (p3) and showed a reduction of RGC viability to 18.5 ± 8.7% after 2 hr in a hypoxia chamber. Schnichels et al. (2017) cultivated whole rat retinae and investigated the reduction of RGCs under 45–120 min of hypoxia, showing a decrease in RGC amount dependent on hypoxia duration and incubation time. After 75 min of hypoxia, approximately 50% of the RGCs died and 15% were apoptotic.

However, our MEA-based hypoxia model has the advantage of not only analyzing the cell survival rate, but also the electrical retinal function prior, during, and after hypoxic conditions.

The gene profiles revealed big differences between the *ex vivo* groups compared to the *in vivo* status, whereas the differences between the *ex vivo* groups themselves were quite small. Only few coding genes were significantly regulated with a FC ≥ 1.25, suggesting no clear differences on transcript level. Compared to the *in vivo* status, several IEGs were significantly upregulated. The upregulation of IEGs indicates a fast and the first response to stimuli like extracellular stress. The top regulated coding gene was the cysteine-rich protein 61 (Cyr61/CCN1). Cyr61 is a secreted and heparin-binding protein encoded by a growth factor-inducible IEG. It is an extracellular matrix-associated signaling molecule, which promotes the adhesion of endothelial cells and stimulates their migration (Babic et al., 1998). It can induce the development of stable retinal blood vessels (Hasan et al., 2011), stimulate revascularization (Fataccioli
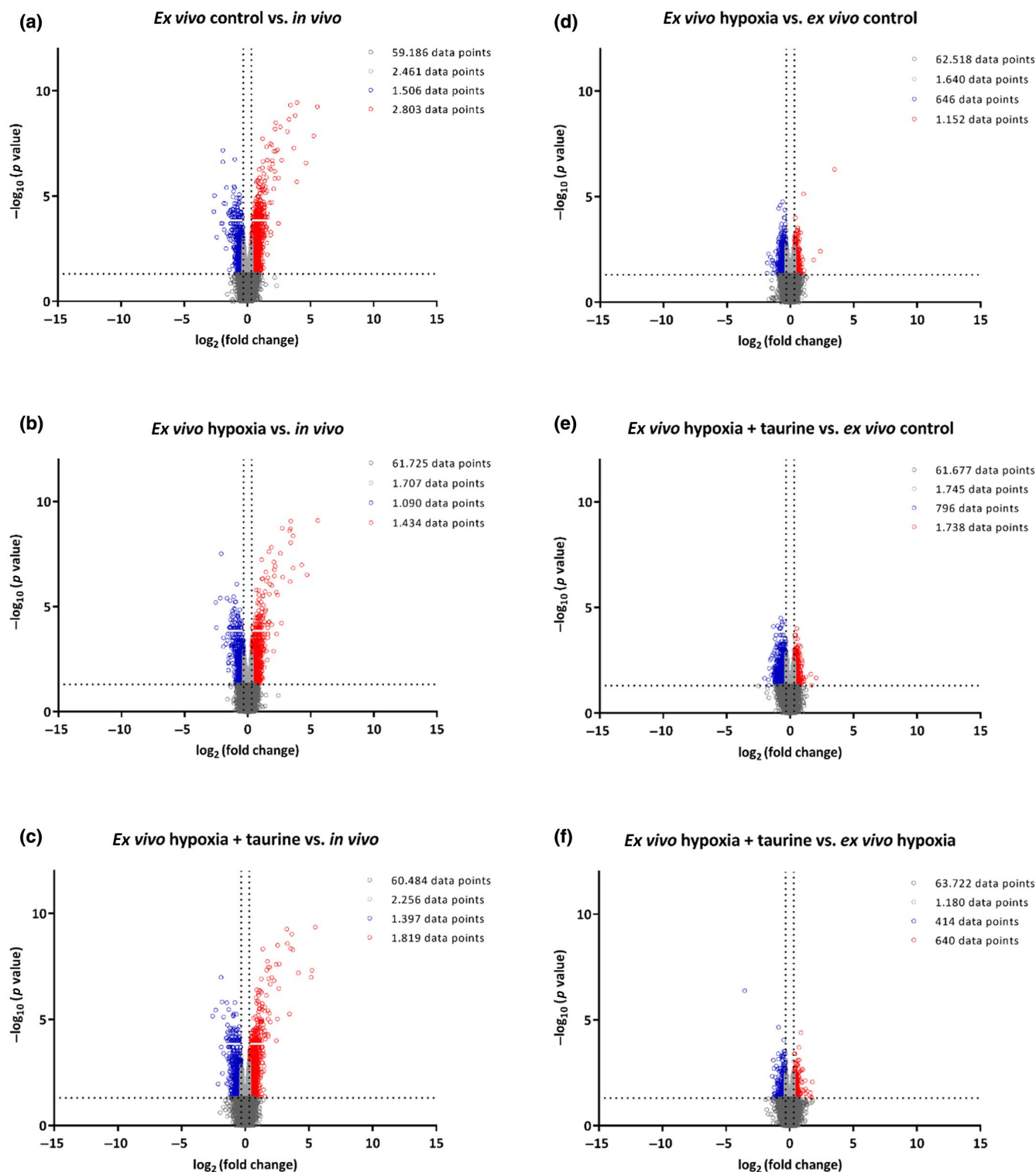
FIGURE 7 Microarray-based analysis of retinal gene expression profiles. The gene expression profiles of retinae under different culture conditions (*in vivo*, *ex vivo* control, *ex vivo* hypoxia, and *ex vivo* hypoxia + taurine) were analyzed using a microarray-based transcriptome-wide gene expression analysis: (a–c) gene expression profiles compared to the *in vivo* status and (d–f) gene expression profiles of the *ex vivo* groups compared to each other. Significantly downregulated genes ($p \leq 0.05$) with a fold change ≤ -1.25 are shown in blue, significantly upregulated genes with a fold change ≥ 1.25 are shown in red, significantly regulated genes with a fold change between -1.25 and 1.25 are shown in light gray. Not significantly regulated genes are shown in dark gray. The data gap between 3.7 and 4.0 in the volcano plots resulted from a p value that was either $p = 0.0002$ ($-\log_{10}(0.0002) = 3.7$) or $p = 0.0001$ ($-\log_{10}(0.0001) = 4.0$). Graphs were generated using GraphPad Prism Software Version 7 [$n_{\text{retina pairs}} = 3$/group] [Color figure can be viewed at wileyonlinelibrary.com]
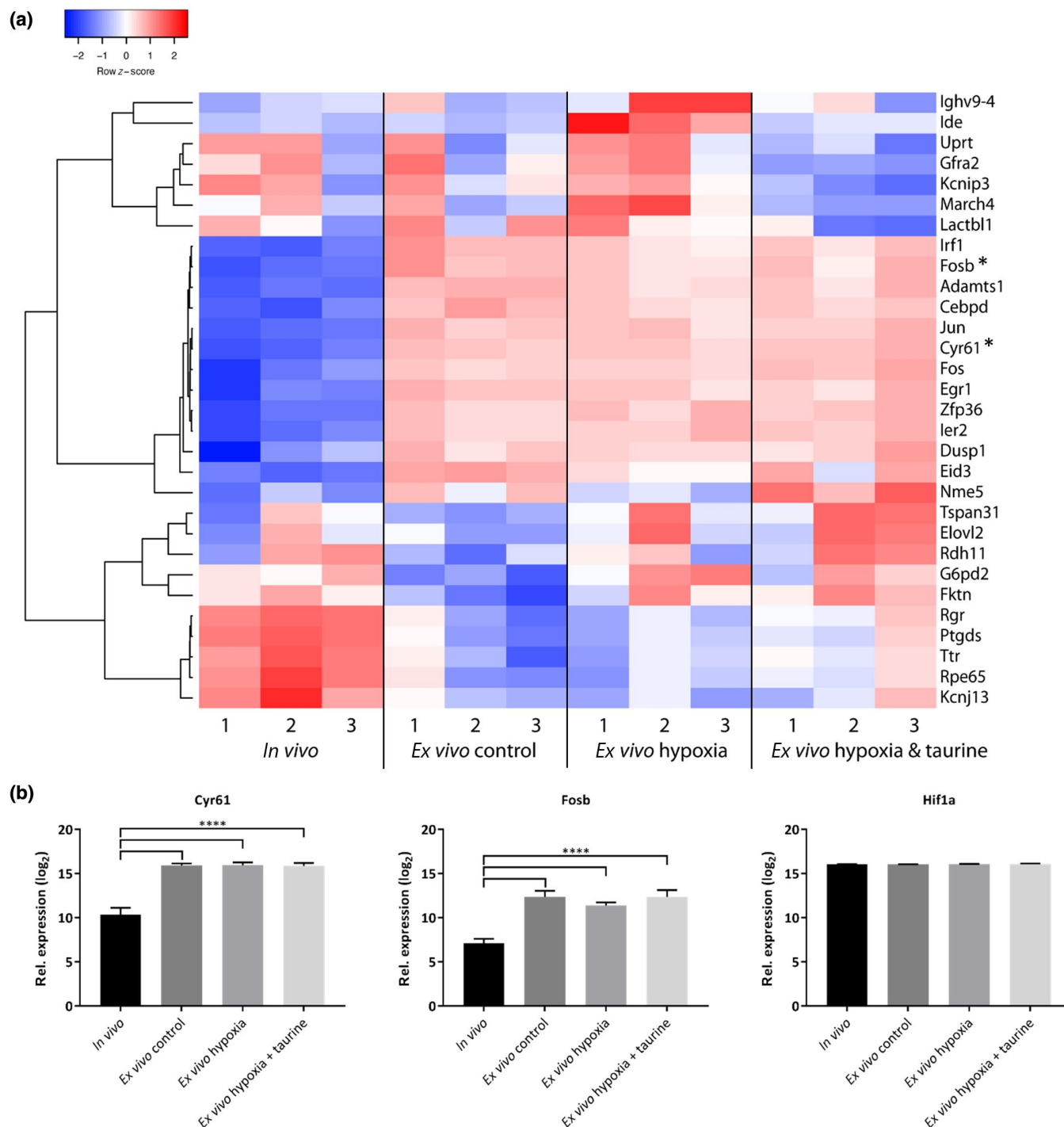
FIGURE 8 Heat map of most regulated coding genes and elected genes in retinae after cultivation under different oxygen conditions. The gene expression profiles of retinae under different culture conditions (*in vivo*, *ex vivo* control, *ex vivo* hypoxia, and *ex vivo* hypoxia + taurine) were analyzed using a microarray-based transcriptome-wide gene expression analysis. (a) Heat map of the most regulated genes showing downregulation in blue and upregulation in red. Expression of the genes marked with asterisks is detailed in (b). (b) The genes *Cyr61* and *Fosb* are strongly upregulated in the *ex vivo* retinae compared to the *in vivo* status. The hypoxia regulated gene *Hif1a* is not significantly regulated. Data are presented as mean ± *SD*. One-way ANOVA was performed using Affymetrix® Transcriptome Analysis Console (TAC) Software [$n_{retina pairs}$ = 3/group] [Color figure can be viewed at wileyonlinelibrary.com]

et al., 2002), and induce neovascularization in rat corneas (Babic et al., 1998). Furthermore, the proto-oncogenes *Fos* (encoding for c-Fos), *Fosb* (FosB/G0/G1 switch regulatory protein 3), and *Jun* (c-Jun) were upregulated in the *ex vivo* groups. Members of the Fos family form heterodimers with members of the Jun family resulting in the formation of the activator protein-1 (AP-1). AP-1 is an early response transcription factor, which converts extracellular signals into changes in gene expression. Those signals can be physiological

stimuli as well as environmental insults, for example, growth factors, cytokines or UV-irradiation (Karin & Shaulian, 2001).

The enrichment analysis revealed reactions to external stress stimuli as well. Our results, indicating a fast and first response to external stress stimuli in all *ex vivo* retinae, show how straining the experiment itself was. Regardless whether hypoxia was induced or not, all *ex vivo* retinae exhibited an increase in IEGs, reinforcing the necessity of appropriate controls. For there were mainly significant differences in gene expression between the *in vivo* and *ex vivo* status, but not between the different *ex vivo* groups, the results suggested that the incubation time was too short to reveal significant changes on transcript level. However, there were reasons why the incubation time was not increased: (a) the treatment of the retinae for the gene expression analysis was chosen according to the timeline of the MEA experiments and (b) an increase in the hypoxic period would have resulted in too many dead cells. In order to accommodate the latency in transcript change, the protocol for the *ex vivo* retinae included a recovery time as well. The preceding analyses of both treatments, with and without recovery, suggested clearer changes in gene expression profiles when a recovery time followed the hypoxic period (data not shown).

Not only the induction of hypoxia, but even slight hypoxic conditions during the preparation or due to artificial perfusion with oxygenated medium can cause reduction in electrical activity, a decreased cell survival as well as an early response to stress, as seen by the emerging activity during lead time in MEA experiments, the amount of dead cells in the *ex vivo* control group of the FDA/PI-stained retinae, and the gene expression profile of the *ex vivo* control retinae, respectively. Thus, therapeutic agents protecting the retina from hypoxia-induced damage have to be delivered fast or even prophylactically. One possible candidate examined here is taurine.

Taurine had no effect on the level of electrical activity returning after hypoxia, but it modulated the RGC response rate after hypoxic stress. The response rate was significantly increased after a hypoxic period of 30 min under taurine. Furthermore, the survival rate of cells in the GCL after hypoxia was higher in the presence of taurine, and also the gene expression profile of the taurine group had more resemblance to the *ex vivo* control than to the hypoxia group. The effects taurine had were moderate, but noticeable throughout all experiments. Our results correspond to other findings, where a positive effect of taurine on the survival rate of cells was reported (Chen et al., 2009; Froger et al., 2012) and the modulation of the pathologic electrical RGC activity in the rd10 mouse model was shown (Schaffrath et al., 2019).

The RGC firing behavior under conventional test conditions has been so diverse and led to a high variability of the control values within this study, making it difficult to gain significant results. Therefore, the positive effect of taurine on the stressed retina has to be examined in more detail, but considered as potential therapeutic for eye diseases associated with hypoxia, for example, glaucoma.

For patients with glaucoma, however, increased intraocular pressure (IOP) is described to be the main risk factor. During glaucoma, hypoxia and increased IOP can account separately as well as in combination for retinal cell damage.

Additionally, our system will be used in future to test the effects of other neuroprotective and neuromodulating agents on the stressed retina. Promising candidates are betaxolol, brimonidine, and pigment epithelium-derived factor (PEDF), which we—in addition to taurine—have already shown to positively affect the electrical RGC activity in rd10 retinae (Schaffrath et al. (2019) and unpublished data). Betaxolol is a selective β1-adrenergic receptor antagonist. It is used for the treatment of hypertension and glaucoma, and is shown to have neuroprotective effects on the ischemic retina (Osborne et al., 1997). Brimonidine (5-bromo-*N*-(4,5-dihydro-1*H*-imidazol-2-yl)quinoxalin-6-amine) is a highly selective α2-adrenergic receptor agonist. WoldeMussie et al. (2001) showed its neuroprotective activity regarding a decreased loss of RGCs in a chronic ocular hypertension rat model. PEDF is a glycoprotein with antiangiogenic, anti-inflammatory, and neuroprotective effects (Tsao et al., 2006; Zhang et al., 2006). In response to hypoxic insult, PEDF counterbalances VEGF, making it a promising therapeutic target for pathologic neovascularization (Mori et al., 2002).

The *ex vivo* hypoxia model established here was able to reproduce findings as well as generate new insights into the effects of hypoxic conditions on the murine wt retina. The results showed the immense impairment of hypoxic stress on the retina, especially on RGCs. However, it also enables the testing of neuroprotective substances and can be used to further investigate promising therapeutic agents for hypoxia-associated retinal diseases.

DECLARATION OF TRANSPARENCY

The authors, reviewers and editors affirm that in accordance to the policies set by the *Journal of Neuroscience Research*, this manuscript presents an accurate and transparent account of the study being reported and that all critical details describing the methods and results are present.

CONFLICT OF INTEREST

The authors have no conflict of interest to disclose.

AUTHOR CONTRIBUTIONS

PEER REVIEW

The peer review history for this article is available at https://publons.com/publon/10.1002/jnr.24899.

DATA AVAILABILITY STATEMENT

All data owned by the authors are available upon request.

ORCID

Sandra Johnen https://orcid.org/0000-0003-0028-2557

REFERENCES

Ames, A., 3rd, & Nesbett, F. B. (1981). In vitro retina as an experimental model of the central nervous system. *Journal of Neurochemistry*, 37(4), 867–877. https://doi.org/10.1111/j.1471-4159.1981.tb04473.x

Arjamaa, O., Aaltonen, V., Piippo, N., Csont, T., Petrovski, G., Kaarniranta, K., & Kauppinen, A. (2017). Hypoxia and inflammation in the release of VEGF and interleukins from human retinal pigment epithelial cells. *Graefes Archive for Clinical and Experimental Ophthalmology*, 255(9), 1757–1762. https://doi.org/10.1007/s00417-017-3711-0

Babic, A. M., Kireeva, M. L., Kolesnikova, T. V., & Lau, L. F. (1998). CYR61, a product of a growth factor-inducible immediate early gene, promotes angiogenesis and tumor growth. *Proceedings of the National Academy of Sciences of the United States of America*, 95(11), 6355–6360. https://doi.org/10.1073/pnas.95.11.6355

Benveniste, H., Drejer, J., Schousboe, A., & Diemer, N. H. (1984). Elevation of the extracellular concentrations of glutamate and aspartate in rat hippocampus during transient cerebral ischemia monitored by intracerebral microdialysis. *Journal of Neurochemistry*, 43(5), 1369–1374. https://doi.org/10.1111/j.1471-4159.1984.tb05396.x

Bernaudin, M., Nedelec, A. S., Divoux, D., MacKenzie, E. T., Petit, E., & Schumann-Bard, P. (2002). Normobaric hypoxia induces tolerance to focal permanent cerebral ischemia in association with an increased expression of hypoxia-inducible factor-1 and its target genes, erythropoietin and VEGF, in the adult mouse brain. *Journal of Cerebral Blood Flow and Metabolism*, 22(4), 393–403. https://doi.org/10.1097/00004647-200204000-00003

Block, F., & Schwarz, M. (1997). Effects of antioxidants on ischemic retinal dysfunction. *Experimental Eye Research*, 64(4), 559–564. https://doi.org/10.1006/exer.1996.0244

Chan, P. H. (1994). Oxygen radicals in focal cerebral ischemia. *Brain Pathology*, 4(1), 59–65. https://doi.org/10.1111/j.1750-3639.1994.tb00811.x

Chen, K. A., Zhang, Q., Wang, J., Liu, F., Mi, M., Xu, H., Chen, F., & Zeng, K. (2009). Taurine protects transformed rat retinal ganglion cells from hypoxia-induced apoptosis by preventing mitochondrial dysfunction. *Brain Research*, 1279, 131–138. https://doi.org/10.1016/j.brainres.2009.04.054

Dreyer, E. B., Zurakowski, D., Schumer, R. A., Podos, S. M., & Lipton, S. A. (1996). Elevated glutamate levels in the vitreous body of humans and monkeys with glaucoma. *Archives of Ophthalmology*, 114(3), 299–305. https://doi.org/10.1001/archopht.1996.01100130295012

El-Sherbeny, A., Naggar, H., Miyauchi, S., Ola, M. S., Maddox, D. M., Martin, P. M., & Smith, S. B. (2004). Osmoregulation of taurine transporter function and expression in retinal pigment epithelial, ganglion, and muller cells. *Investigative Ophthalmology & Visual Science*, 45(2), 694–701.

Fabregat, A., Sidiropoulos, K., Viteri, G., Forner, O., Marin-Garcia, P., Arnau, V., D'Eustachio, P., Stein, L., & Hermjakob, H. (2017). Reactome pathway analysis: A high-performance in-memory approach. *BMC Bioinformatics*, 18(1), 142. https://doi.org/10.1186/s12859-017-1559-2

Fataccioli, V., Abergel, V., Wingertsmann, L., Neuville, P., Spitz, E., Adnot, S., Calenda, V., & Teiger, E. (2002). Stimulation of angiogenesis by Cyr61 gene: A new therapeutic candidate. *Human Gene Therapy*, 13(12), 1461–1470. https://doi.org/10.1089/10430340260185094

Froger, N., Cadetti, L., Lorach, H., Martins, J., Bemelmans, A.-P., Dubus, E., Degardin, J., Pain, D., Forster, V., Chicaud, L., Ivkovic, I., Simonutti, M., Fouquet, S., Jammoul, F., Léveillard, T., Benosman, R., Sahel, J.-A., & Picaud, S. (2012). Taurine provides neuroprotection against retinal ganglion cell degeneration. *PLoS ONE*, 7(10), e42017. https://doi.org/10.1371/journal.pone.0042017

Fukumura, D., Gohongi, T., Kadambi, A., Izumi, Y., Ang, J., Yun, C.-O., Buerk, D. G., Huang, P. L., & Jain, R. K. (2001). Predominant role of endothelial nitric oxide synthase in vascular endothelial growth factor-induced angiogenesis and vascular permeability. *Proceedings of the National Academy of Sciences of the United States of America*, 98(5), 2604–2609. https://doi.org/10.1073/pnas.041359198

Gross, R. L., Hensley, S. H., Gao, F., & Wu, S. M. (1999). Retinal ganglion cell dysfunction induced by hypoxia and glutamate: Potential neuroprotective effects of β-blockers. *Survey of Ophthalmology*, 43, 162–170. https://doi.org/10.1016/S0039-6257(99)00054-5

Hasan, A., Pokeza, N., Shaw, L., Lee, H.-S., Lazzaro, D., Chintala, H., Rosenbaum, D., Grant, M. B., & Chaqour, B. (2011). The matricellular protein cysteine-rich protein 61 (CCN1/Cyr61) enhances physiological adaptation of retinal vessels and reduces pathological neovascularization associated with ischemic retinopathy. *Journal of Biological Chemistry*, 286(11), 9542–9554. https://doi.org/10.1074/jbc.M110.198689

Hong, S., Lee, J. E., Kim, C. Y., & Seong, G. J. (2007). Agmatine protects retinal ganglion cells from hypoxia-induced apoptosis in transformed rat retinal ganglion cell line. *BMC Neuroscience*, 8, 81. https://doi.org/10.1186/1471-2202-8-81

Ikeda, E., Achen, M. G., Breier, G., & Risau, W. (1995). Hypoxia-induced transcriptional activation and increased mRNA stability of vascular endothelial growth factor in C6 glioma cells. *Journal of Biological Chemistry*, 270(34), 19761–19766. https://doi.org/10.1074/jbc.270.34.19761

Irizarry, R. A., Bolstad, B. M., Collin, F., Cope, L. M., Hobbs, B., & Speed, T. P. (2003). Summaries of Affymetrix GeneChip probe level data. *Nucleic Acids Research*, 31(4), e15. https://doi.org/10.1093/nar/gng015

Janaky, M., Grosz, A., Toth, E., Benedek, K., & Benedek, G. (2007). Hypobaric hypoxia reduces the amplitude of oscillatory potentials in the human ERG. *Documenta Ophthalmologica*, 114(1), 45–51. https://doi.org/10.1007/s10633-006-9038-5

Jeon, C. J., Strettoi, E., & Masland, R. H. (1998). The major cell populations of the mouse retina. *Journal of Neuroscience*, 18(21), 8936–8946. https://doi.org/10.1523/JNEUROSCI.18-21-08936.1998

Jo, N., Wu, G. S., & Rao, N. A. (2003). Upregulation of chemokine expression in the retinal vasculature in ischemia-reperfusion injury. *Investigative Ophthalmology & Visual Science*, 44(9), 4054–4060. https://doi.org/10.1167/iovs.02-1308

Karin, M., & Shaulian, E. (2001). AP-1: Linking hydrogen peroxide and oxidative stress to the control of cell proliferation and death. *IUBMB Life*, 52(1–2), 17–24. https://doi.org/10.1080/15216540252774711

Kaur, C., Sivakumar, V., & Foulds, W. S. (2006). Early response of neurons and glial cells to hypoxia in the retina. *Investigative Ophthalmology & Visual Science*, 47(3), 1126–1141. https://doi.org/10.1167/iovs.05-0518

Kaur, C., Sivakumar, V., Yong, Z., Lu, J., Foulds, W. S., & Ling, E. A. (2007). Blood-retinal barrier disruption and ultrastructural changes in the hypoxic retina in adult rats: The beneficial effect of melatonin administration. *Journal of Pathology*, *212*(4), 429–439. https://doi.org/10.1002/path.2195

Kergoat, H., Herard, M. E., & Lemay, M. (2006). RGC sensitivity to mild systemic hypoxia. *Investigative Ophthalmology & Visual Science*, *47*(12), 5423–5427. https://doi.org/10.1167/iovs.06-0602

Levy, A. P., Levy, N. S., Wegner, S., & Goldberg, M. A. (1995). Transcriptional regulation of the rat vascular endothelial growth factor gene by hypoxia. *Journal of Biological Chemistry*, *270*(22), 13333–13340. https://doi.org/10.1074/jbc.270.22.13333

Louzada, P. R., Paula Lima, A. C., Mendonca-Silva, D. L., Noel, F., De Mello, F. G., & Ferreira, S. T. (2004). Taurine prevents the neurotoxicity of beta-amyloid and glutamate receptor agonists: Activation of GABA receptors and possible implications for Alzheimer's disease and other neurological disorders. *FASEB Journal*, *18*(3), 511–518. https://doi.org/10.1096/fj.03-0739com

Macaione, S., Ruggeri, P., De Luca, F., & Tucci, G. (1974). Free amino acids in developing rat retina. *Journal of Neurochemistry*, *22*, 887–891. https://doi.org/10.1111/j.1471-4159.1974.tb04313.x

Martin, G., Conrad, D., Cakir, B., Schlunck, G., & Agostini, H. T. (2018). Gene expression profiling in a mouse model of retinal vein occlusion induced by laser treatment reveals a predominant inflammatory and tissue damage response. *PLoS ONE*, *13*(3), e0191338. https://doi.org/10.1371/journal.pone.0191338

Mori, K., Gehlbach, P., Ando, A., McVey, D., Wei, L., & Campochiaro, P. A. (2002). Regression of ocular neovascularization in response to increased expression of pigment epithelium-derived factor. *Investigative Ophthalmology & Visual Science*, *43*(7), 2428–2434.

Neo, T., Gozawa, M., Takamura, Y., Inatani, M., & Oki, M. (2020). Gene expression profile analysis of the rabbit retinal vein occlusion model. *PLoS ONE*, *15*(7), e0236928. https://doi.org/10.1371/journal.pone.0236928

Osborne, N. N., Casson, R. J., Wood, J. P., Chidlow, G., Graham, M., & Melena, J. (2004). Retinal ischemia: Mechanisms of damage and potential therapeutic strategies. *Progress in Retinal and Eye Research*, *23*(1), 91–147. https://doi.org/10.1016/j.preteyeres.2003.12.001

Osborne, N. N., Cazevieille, C., Carvalho, A. L., Larsen, A. K., & DeSantis, L. (1997). In vivo and in vitro experiments show that betaxolol is a retinal neuroprotective agent. *Brain Research*, *751*, 113–123. https://doi.org/10.1016/S0006-8993(96)01393-5

Pasantes-Morales, H., & Ordonez, A. (1982). Taurine activation of a bicarbonate-dependent, ATP-supported calcium uptake in frog rod outer segments. *Neurochemical Research*, *7*(3), 317–328. https://doi.org/10.1007/BF00965643

Schaffrath, K., Diarra, S., Gehlen, J., Muller, F., Walter, P., & Johnen, S. (2019). Modulation of the electrical activity in degenerative retinas of rd10 mice using neuroprotective drugs. *Investigative Ophthalmology & Visual Science*, *60*(9), 20.

Schnichels, S., Blak, M., Hurst, J., Dorfi, T., Bartz-Schmidt, K. U., Ziemssen, F., Spitzer, M. S., & Schultheiss, M. (2017). Establishment of a retinal hypoxia organ culture model. *Biology Open*, *6*(7), 1056–1064. https://doi.org/10.1242/bio.025429

Szabo, M. E., Droy-Lefaix, M. T., & Doly, M. (1997). Direct measurement of free radicals in ischemic/reperfused diabetic rat retina. *Clinical Neuroscience*, *4*(5), 240–245.

Tan, J., Ye, X., Xu, Y., Wang, H., Sheng, M., & Wang, F. (2011). Acid-sensing ion channel 1a is involved in retinal ganglion cell death induced by hypoxia. *Molecular Vision*, *17*, 3300–3308.

Tsao, Y. P., Ho, T. C., Chen, S. L., & Cheng, H. C. (2006). Pigment epithelium-derived factor inhibits oxidative stress-induced cell death by activation of extracellular signal-regulated kinases in cultured retinal pigment epithelial cells. *Life Sciences*, *79*(6), 545–550. https://doi.org/10.1016/j.lfs.2006.01.041

Van Bergen, N. J., Wood, J. P. M., Chidlow, G., Trounce, I. A., Casson, R. J., Ju, W.-K., Weinreb, R. N., & Crowston, J. G. (2009). Recharacterization of the RGC-5 retinal ganglion cell line. *Investigative Ophthalmology & Visual Science*, *50*(9), 4267–4272. https://doi.org/10.1167/iovs.09-3484

Winkler, B. S. (1981). Glycolytic and oxidative metabolism in relation to retinal function. *Journal of General Physiology*, *77*(6), 667–692. https://doi.org/10.1085/jgp.77.6.667

WoldeMussie, E., Ruiz, G., Wijono, M., & Wheeler, L. A. (2001). Neuroprotection of retinal ganglion cells by brimonidine in rats with laser-induced chronic ocular hypertension. *Investigative Ophthalmology & Visual Science*, *42*(12), 2849–2855.

Zhang, S. X., Wang, J. J., Gao, G., Shao, C., Mott, R., & Ma, J. X. (2006). Pigment epithelium-derived factor (PEDF) is an endogenous antiinflammatory factor. *FASEB Journal*, *20*(2), 323–325. https://doi.org/10.1096/fj.05-4313fje

SUPPORTING INFORMATION

Additional Supporting Information may be found online in the Supporting Information section.

Transparent Science Questionnaire for Authors

Transparent Peer Review Report